

A statistical analysis for the characteristics of cloud/precipitation system from Cloudsat data

Munehisa K. Yamamoto, Atsushi Higuchi, and Masamitsu Hayasaki

Center for Environmental Remote Sensing, Chiba University, Japan, mkyamamoto@faculty.chiba-u.jp

Abstract

Global distributions of cloud largely effect earth radiation budgets. The heating / cooling effect differs depending on a type of cloud due to the differences of the characteristics of radiative process. Thus, it is important to understand cloud distributions classified into some cloud types. A cloud type classification method has been developed using multiple bands in visible and infrared using geostationary satellite. However, it was hard to classify the cloud types because of limit of information from optical thickness and cloud top height.

In 2006, Cloudsat satellite carrying the Cloud Profiling Radar (CPR) was launched, and its observation enables us to find vertical distributions of cloud globally. This study tried to characterize cloud / precipitation characteristics and classify cloud types from vertical distributions of clouds observed by Cloudsat CPR. This study applied a base of vertical-method of the Tropical Rainfall Measuring Mission (TRMM) Precipitation Radar (PR) 2A23 algorithm to the vertical distributions of reflectivity factor (Z) from CPR in order to detect the bright band height (BBH) and cloud types. The detected BBH exists under 250-500 m from freezing height derived from a re-analysis data. The cloud types were classified into convective with large Z, stratiform with BBH, and others.

In this presentation, we will also report the characteristics of global cloud distributions with / without precipitation, with shallow or anvil, and so on.

Keywords : Remote sensing, Cloudsat CPR, cloud distribution

1. Introduction

Recently, the global warming attracts big attention. One of the biggest concerns is the change of the global cloud distributions. Global distributions of cloud largely effect earth radiation budgets. The heating / cooling effect differs depending on a type of cloud due to the differences of the characteristics of radiative process such as reflection from short wave radiation and absorption and emission from long wave radiation. Since these processes depend on a cloud thickness and cloud temperature, it makes difficult to estimate and predict the global radiation budget. Therefore, it is important to understand cloud distributions classified into the cloud types.

A cloud type classification method has been suggested using multiple bands in visible and infrared using geostationary and low-orbit satellites. For example, Inoue (1987) developed a simple cloud type classification based on split-window technique. Brightness temperature difference between visible and infrared channels has good relation to some cloud types. However, it was hard to classify the cloud types because of limit of information from optical thickness and cloud top height. Using precipitation radar technique, on the other hand, rain type classification method has been developed to estimate precipitation because drop size distributions are largely different with rain types. The

Tropical Rainfall Measuring Mission (TRMM) provides standard products of rain characteristics from three-dimensional radar reflectivity. In 2006, Cloudsat satellite carrying the Cloud Profiling Radar (CPR) was launched, and its observation enables us to find vertical distributions of cloud globally. This study tried to characterize cloud / precipitation characteristics and classify cloud types from vertical distributions of clouds observed by Cloudsat CPR.

This study presents the characteristics of global cloud precipitation distributions and the classification of cloud types from Cloudsat CPR.

2. Data

This study mainly used Cloudsat CPR 2B-GEOPROF product provided by the Cloudsat Data Processing Center for June-July August (JJA) 2007–2009. This product provides radar reflectivity factor and significant echo and cloud flag observed by CPR, MODIS, and ECMWF data. In order to compare the simultaneous observation data between Cloudsat CPR and TRMM PR, we used 2D-CLOUDSAT-TRMM product. This product summarizes a basic nearest-neighbor interpolation of the TRMM data on to the Cloudsat data's along track resolution, and generated for intersects with an overpass time difference of 50 minute or less.

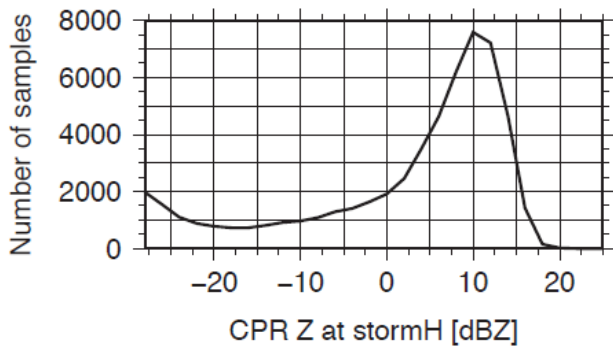


Fig. 1 Appearance number of CPR radar reflectivity factor at TRMM stormH.

3. Results

3.1 Instantaneous Cloudsat CPR vs TRMM PR

Radar reflectivity factor Z is given by the sixth-powers of the diameters of all the drops contained in a unit volume of space. However, equivalent radar reflectivity factor (Z_e), Z derived from radar received power, is affected by precipitation attenuation depending on radar frequency. Under the simultaneous observation, Z_e from Cloudsat CPR and TRMM PR should be different value. When storm top height (stormH as the top height of precipitation) is identified from Cloudsat CPR, this difference must be considered. According to the appearance number of Cloudsat CPR Z_e at the stormH from TRMM PR (about 17 dBZ) in the simultaneous observations (Fig. 1), Z_e is concentrated around 10 dBZ. This difference is explained by the radar frequency, horizontal resolutions, and overpass time difference. From this result, hereafter stormH from Cloudsat CPR is defined by the top height of 10 dBZ.

Figure 2 shows the appearance frequency of radar echo from Cloudsat CPR and TRMM PR at the same pixel. When both of the echoes are detected in the pixel, cloud with precipitation would exist. If the Cloudsat CPR only observes radar echo, this pixel would contain non-precipitating cloud. There are few pixels just TRMM PR echo detected. Over 90% of the radar echo detected pixels exists non-precipitating clouds except for tropics. The appearance frequency of precipitating clouds in the tropics is higher than those in the mid-latitude regions. This implies that shallow and weak precipitation frequently occurs in the mid-latitude ocean.

3.2 Global distributions of cloud / precipitation parameters

Historically cloud type and cloud top height detections from satellite sensors have been used by visible and infrared

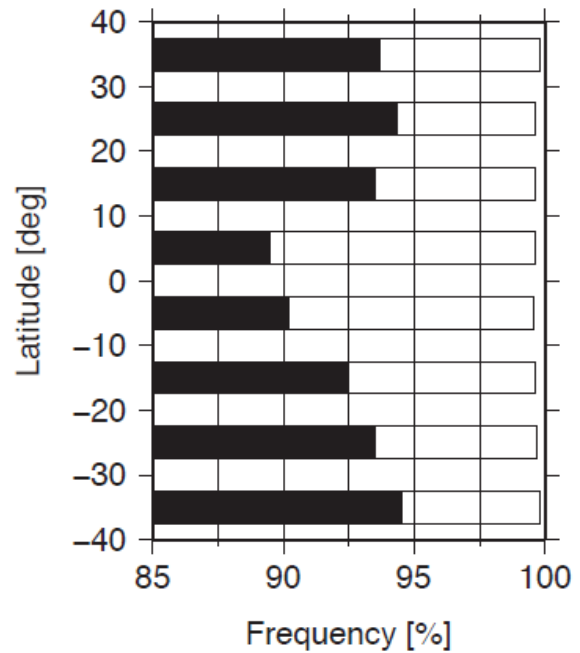


Fig. 2 Appearance frequency of cloud / rain detected pixels with Cloudsat CPR (black) and with both CPR and TRMM PR (white) displayed by cumulative bar chart.

channels. However, it is hard to estimate them precisely due to lack of vertical resolutions. Moreover, it is not easy task to match up simultaneous data of both of cloudH and stormH unless TRMM PR and VIRS observations. Assuming the correspondence of stormH from Cloudsat CPR mentioned the precious subsections, relationship between stormH and cloudH should be further understood.

Figure 3a shows mean cloudH from Cloudsat CPR. Over ocean, cloudH over 12 km appears over the maritime continent, the Bay of Bengal, and the west coast of the Mexico. High cloudH regions correspond to large amount of rainfall. Over land, cloudH also exceed 10 km over tropical Africa and south-east Asia. However, cloudH over land is generally lower than that over ocean. From the difference between the ascending and descending passes (Fig. 3b), cloudH over ocean (land) in the early-afternoon pass is higher (lower) than that in the mid-night pass due to diurnal variations of cloud activity. Mean stormH distributions (Fig. 3c) apparently similar to the mean cloudH. However, high stormH regions are relatively different particularly over land (e.g. the Tibetan Plateau, western India, and North America). The ascending-descending contrast between land and ocean is apparently obscured, but stormH over the Rocky Mountains is dominant in nighttime. These diurnal variations correspond to those from TRMM PR and VIRS (Yamamoto et al. 2008).

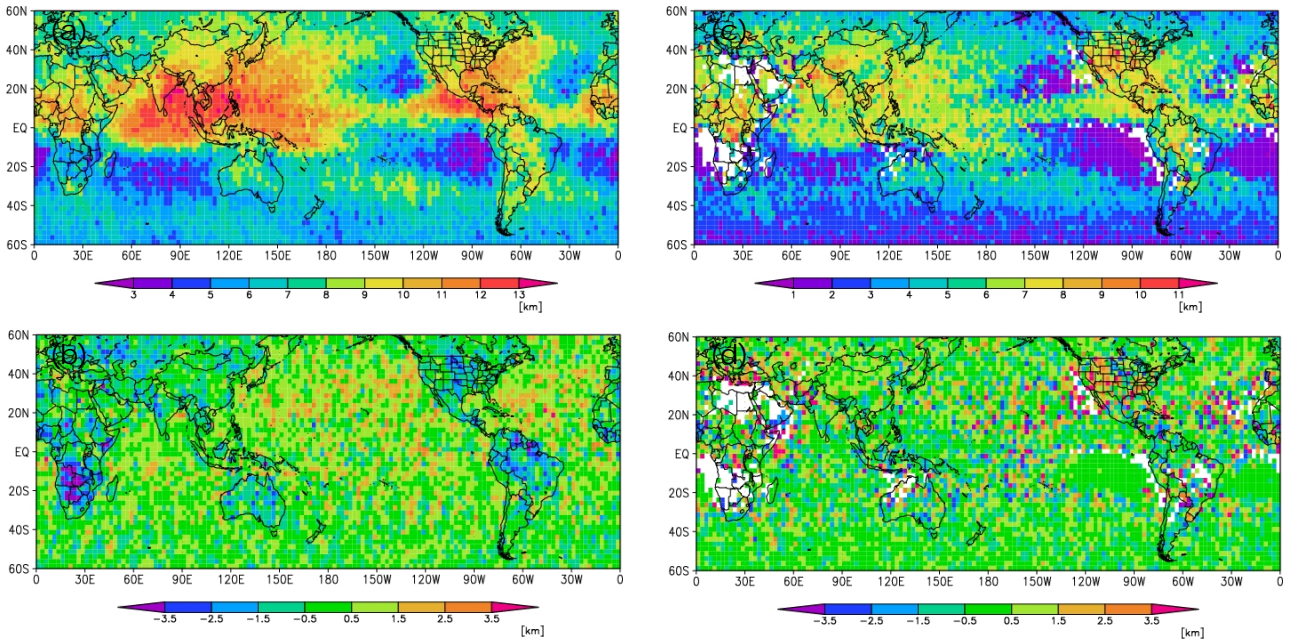


Fig. 4 Horizontal distributions of (a) Mean cloudH in the daily passes (b) difference of mean cloudH between the daily pass and nocturnal pass, and (c) (d) those for mean stormH observed by Cloudsat CPR in 2007-2009 JJA.

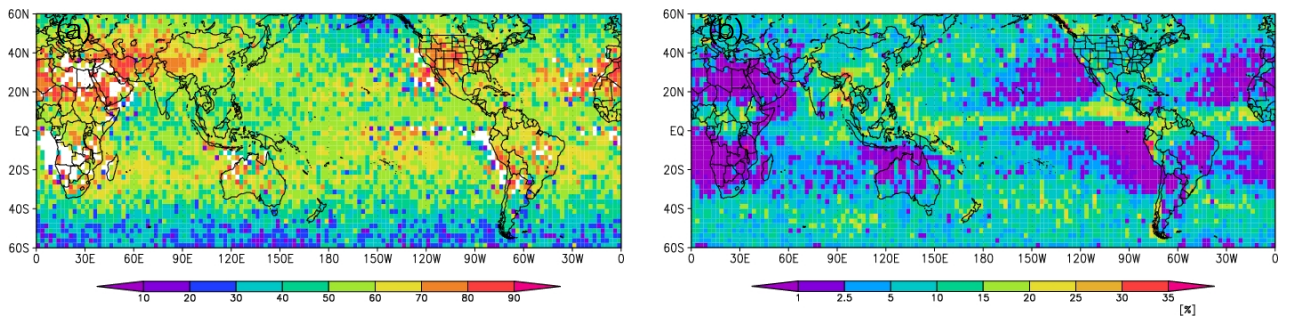


Fig. 5 Horizontal distributions of (a) median of stormH / cloudH and (b) occurrence frequency in stormH / cloudH in the daily pass observed by Cloudsat CPR in 2007-2009 JJA.

Frequency of occurrence with stormH to cloudH is shown in Fig. 4. The high frequency regions where cloud system is likely to cause precipitation occur over the Bay of Bengal and the west coast of Mexico. Over the mid-latitude region, large differences of the frequency are not found.

As convective system develops, storm height generally increases. A ratio of stormH to cloudH would be one of the indices of convective activity. Figure 4 illustrates median of all pixels with stormH / cloudH. StormH reaches above 80% of cloudH in the Sahara, Middle-east, the Tibetan Plateau, and Rocky Mountains. Over ocean, tropic region becomes higher ratio than in mid-latitude. Regions with relatively the high ratio such as south Indian Ocean and south-east Pacific correspond to small precipitation amount.

3.3 Cloud type classification from Cloudsat CPR

In order to identify further cloud / precipitation

characteristics, a classification method based on the V-method of TRMM PR2A23 algorithm (Awaka 2007) was applied to the Cloudsat CPR data except for some modifications (Table 1). For the freezing height estimation vertical distributions of temperature and geopotential height from the Japanese 25-year Reanalysis (JRA-25) and JMA Climate Data Assimilation System (JCDAS) data instead of monthly mean surface temperature and constant lapse rate.

Figure 6 shows vertical distributions of radar echoes with freezH, BBH, and cloud type observed by Cloudsat CPR and those observed by TRMM PR at a case of overpass. BBH exists under 250-500m from freezH with small variations. From the vertical distributions of radar echoes BBH is reasonably detected. Compared to the rain type from TRMM PR, further cloud type characteristics are detected due to finer resolution.

In the cloud type classification by infrared sensors, it is

Table 1 Parameters from Cloudsat CPR developed in this study and modifications from PR2A23 standard product.

TRMM PR	Cloudsat CPR	Modification
rainFlag	cloudFlag	Cloud certain / possible was identified from CPR_Cloud_mask
rainType	cloudType	V-method was only applied to cloudType. Convective cloud was identified from Zmax > 15 dBZ
freezH	freezH	JRA25 data instead of monthly mean surface temperature
HBB	HBB	freezH1km, Zmax > 10 dBZ
stormH	cloudH	The highest altitude of CPR_Cloud_mask

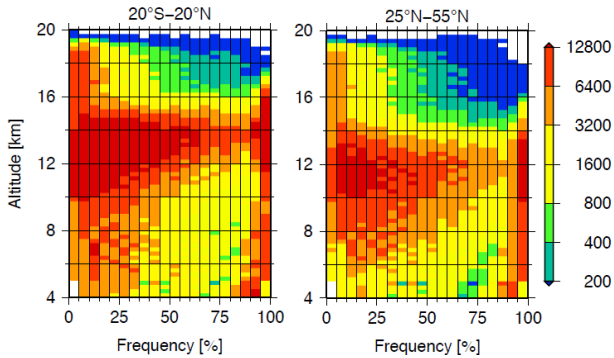


Fig. 3 Contoured appearances of altitude diagram of fulfillment ratio from cloudH observed by Cloudsat CPR in 2008 over ocean in 20°S–20°N (left) and 25°–55°N (right).

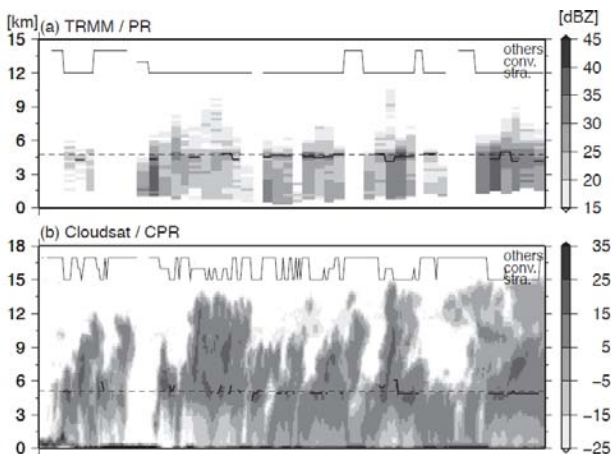


Fig. 6 Vertical distributions of radar reflectivity factor in (a) TRMM PR and (b) Cloudsat CPR (gray image), freezH (dotted lines), bright band height (bold solid lines), and rain (cloud) type (solid line in the upper part of each panel) over 16° N and 96° E at 19:25UTC overpass in 1 September, 2007.

hard to distinguish between cirrus and cumulus cloud due to similar low brightness temperature from high cloudH. On the contrary, since cloud radar can detect vertical distributions of cloud echoes, their classification would be easier. Figure 5 shows relationship between cloudH and fulfillment ratio of radar echo from the surface. Over the tropical ocean (Fig. 5a), large amount of pixels concentrates

less than 30% and more than 90% of fulfillment ratio regardless of the cloudH. 10-14 km of cloudH, corresponding to the tropopause, fulfillment ratio has large variations. These distributions are similar to that over the mid-latitude oceans except for lower cloudH shifts.

4. Summaries

This study investigated cloudH and stormH characteristics from Cloudsat CPR. Compared to the TRMM PR and VIRS observations, more accurate relationship are obtained particularly in cloudH owing to 2-dimensional (vertical) observation. Moreover, drop size distributions, attenuation from precipitation and cloud will be clarified by proceeding to the comparison.

Acknowledgements

This symposium is sponsored by the Ministry of Education, Science, Sports and Culture, Japan (MEXT), and National University Corporation Chiba University.

References

- Awaka, J., T. Iguchi, and K. Okamoto (2007): Rain type classification algorithm. V. Levizzani, P. Bauer, and F. J. Turk (ed.), *Measuring Precipitation from Space EURAINSAT and the Future, Advances in Global Change Research*, 28, Springer, 213-224.
- Inoue, T. (1987): A cloud type classification with NOAA 7 split-window measurements. *J. Geophys. Res.* 92, D4, 3991-4000.
- Onogi, K. and co-authors (2007): The JRA-25 Reanalysis. *J. Meteor. Soc. Japan*, 85, 369-432.
- Yamamoto, M. K., F. A. Furuzawa, A. Higuchi, and K. Nakamura (2008): Comparison of diurnal variations in precipitation systems observed by TRMM PR, TMI, and VIRS. *J. Climate*, 21, 4011-4028.